HHS Public Access

Author manuscript

Curr Opin Colloid Interface Sci. Author manuscript; available in PMC 2019 July 01.

Published in final edited form as:

Curr Opin Colloid Interface Sci. 2018 July ; 36: 58–69. doi:10.1016/j.cocis.2018.01.001.

Surfactant-induced Marangoni transport of lipids and therapeutics within the lung

Amy Z. Stetten[a], **Steven V. Iasella**[d], **Timothy E. Corcoran**[b], **Stephen Garoff**[a,*], **Todd M. Przybycien**[c,d], and **Robert D. Tilton**[c,d]

[a]Carnegie Mellon Center for Complex Fluids Engineering, Department of Physics, Carnegie Mellon University, Pittsburgh, PA 15213, USA

[b]Department of Medicine, University of Pittsburgh, Pittsburgh, PA 15260, USA

[c]Carnegie Mellon Center for Complex Fluids Engineering, Department of Biomedical Engineering, Carnegie Mellon University, Pittsburgh, PA 15213, USA

[d]Carnegie Mellon Center for Complex Fluids Engineering, Department of Chemical Engineering, Carnegie Mellon University, Pittsburgh, PA 15213, USA

Abstract

Understanding the fundamentals of surface transport on thin viscous films has important application in pulmonary drug delivery. The human lung contains a large-area interface between its complex fluid lining and inhaled air. Marangoni flows driven by surface tension gradients along this interface would promote enhanced distribution of inhaled therapeutics by carrying them from where they are deposited in the upper airways, along the fluid interface to deeper regions of the lung. Motivated by the potential to improve therapies for acute and chronic lung diseases, we review recent progress in modeling and experimental studies of Marangoni transport induced by the deposition of surfactant-containing microliter drops and liquid aerosols (picoliter drops) onto a fluid interface. The roles of key system variables are identified, including surfactant solubility, drop miscibility with the subphase, and the thickness, composition and surface properties of the subphase liquid. Of particular interest is the unanticipated but crucial role of aerosol processing to achieve Marangoni transport via phospholipid vesicle dispersions, which are likely candidates for a biocompatible delivery system. Progress in this field has the potential to not only improve outcomes in patients with chronic and acute lung diseases, but also to further our understanding of surface transport in complex systems.

Graphical abstract

*Corresponding Author: sg2e@andrew.cmu.edu.

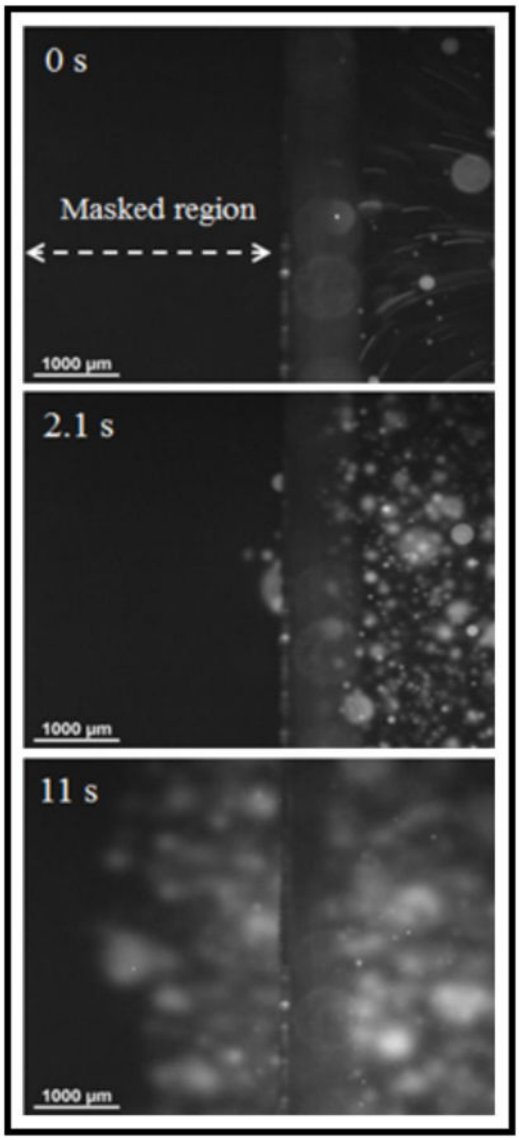

Keywords

Pulmonary drug delivery; Marangoni Flow; Surfactant spreading; Lung Phospholipids; Surfactant Replacement Therapy; Aerosol; Lung mechanics

1. Motivation

Marangoni transport has broad relevance in a wide variety of systems. One such system is the fluid lining in the human lung. The lung is of particular interest because its lining consists of a very large area, complex fluid film whose composition varies with position in the lung and with a person's physiological state. A better understanding of capillary and transport phenomena within this system could lead to improved treatment of chronic and acute lung diseases through improved delivery of pulmonary medications. Recent work has

shown great advances in the science and development of Marangoni-enhanced pulmonary delivery strategies coming from biology, medicine, chemical engineering, and physics.

1.1 Lung diseases treated by direct delivery of medication into the lung

In this article, we will discuss two specific conditions treated by direct delivery of medication into the lung. The first, to be discussed briefly, are diseases that affect production of pulmonary surfactant, and the second, to be discussed more thoroughly, are diseases that cause pathological changes in the mucus of the upper lung airways.

A basic understanding of the structure of the lung will be helpful at this point. The fluid lining of the human lung airways, called the "airway surface liquid" (ASL), is a complex, multicomponent system. The ASL is composed of two layers: 1) a ~ 10 μm thick periciliary liquid (PCL), which is an aqueous layer that resides on the surface of the airway epithelium and contains active cilia, and 2) a 10 – 70 μm thick viscoelastic mucus layer residing atop the PCL, which is composed of 95% water, 2% glycoproteins, 1% lipids and 1% inorganic salts [1–4]. The glycoproteins are referred to as mucins [1,2,6–8]. Some "embedded" mucins are also attached to the cilia themselves within the PCL. The cilia in the PCL are active and "beat" in tandem, causing the mucus layer of the ASL to flow up and out of the lungs to clear particulates and bacteria (mucociliary clearance) [5]. Mucins impart non-Newtonian properties to the fluid that promote mucociliary clearance [6]. One way to model this system would be to treat the mucus layer as a non-Newtonian fluid while treating the PCL as a porous network or "Brinkman fluid" [7,8].

In the small airways beyond generation 15 or 16, there are fewer mucin-producing cells and few to no ciliated cells. Here, the ASL becomes a single layer consisting of a Newtonian aqueous solution with a surface layer of adsorbed pulmonary surfactant. This pulmonary surfactant consists of approximately 90% phospholipids and 10% proteins and serves to reduce the surface tension at the air-water interface of the alveoli and to allow for easier reopening of airways closed upon expiration [9]. The surface tension of the ASL is not well understood and varies spatially in the lung as well as from patient to patient. Many groups have tried different experimental methods to determine ASL surface tension, but the range reported is extremely large, ranging from 5 to 90 mN/m [10–15]. For the purpose of this review, we will consider the commonly quoted experimental values in the range of 20–40 mN/m.

The smaller branching airways terminate in alveolar sacs made up of many alveoli. It is in these alveoli that primary gas exchange occurs. Like the small airways, the alveoli are coated in a Newtonian fluid consisting primarily of saline and aqueous pulmonary surfactant. As the alveolar radii expand and contract from ~ 0.01 mm to ~ 0.05 mm with the breathing cycle, their surface areas increase and decrease dramatically [16]. This likely leads to dramatic changes in alveolar surface tensions from ~ 30 mN/m on inhalation to nearly 0 mN/m on exhalation (an active research topic pursued by Zasadzinski, Franses, and others [17–20]). The pulmonary surfactant within the alveoli functions to reduce the total pressure required to expand the lungs. Laplace's law states that the pressure difference between the inside and the outside of a spherical interface is proportional to the surface tension of that interface. Thus, reducing the surface tension by an order of magnitude (from that of water,

72 mN/m, down to values below 10 mN/m) allows for an order of magnitude decrease in the pressure required to expand the alveoli.

In lung diseases such as infant respiratory distress syndrome (IRDS), the lung does not produce enough pulmonary surfactant. Without this crucial surface tension-reducing agent, it becomes difficult for these patients to inflate their lungs [21]. Currently, IRDS is treated with respiratory support including bolus delivery of surfactant replacement therapy (SRT) formulations, multi-component aqueous dispersions of purified lung surfactant from animals that act to lower the surface tension within the lung and, especially, the alveoli. Inhaled aerosol delivery of SRTs has been performed experimentally [9,22]. Bolus SRT delivery is an effective treatment for infants, however it does not seem to be effective for adults with acute respiratory distress syndrome (ARDS) whether the SRT liquid is delivered by bolus or aerosol [23].

In cystic fibrosis (CF), an obstructive lung disease, airway mucus becomes dehydrated and viscous and, as a result, cannot be cleared effectively [24]. Accumulated mucus becomes a harbor for bacterial infection and mucus plaques that may limit local ventilation [25,26]. Despite prevalent use of prophylactic inhaled antibiotics [26–29], the leading cause of mortality in CF is still opportunistic bacterial infection in the lungs [26,30]. With current inhaled therapies, drug distribution is determined entirely by aerodynamics. Inhaled aerosols follow the airflow, the path of least resistance through the airways. Changes in flow direction or velocity may cause inertial aerosol deposition. These effects are common in the upper airways and become more pronounced when the airways are partially obstructed. [31]. In CF this can lead to increased aerosol deposition in more proximal airways and at airway branch points, often leaving downstream regions of the lung untreated. With these infected areas not receiving adequate treatment, the bacterial infections may persist and possibly become antibiotic resistant [32].

1.2 Marangoni transport for enhanced treatment of lung diseases

The lung disease types described above, as well as any obstructive lung disease, would benefit from the ability to deliver inhaled therapeutic agents deeper and more homogeneously into the lung, to reach more sites of disease. One possible avenue for this improvement is through Marangoni transport, as suggested in a number of references, for example [33–35].

Marangoni transport is a convective surface flow that occurs when there is a gradient in surface tension along an interface. This gradient causes shear stress along the interface, which induces fluid motion from areas of low surface tension to areas of high surface tension. The fluid velocity is proportional to the surface tension gradient. A common example occurs when a drop containing a surface-active agent (surfactant) is deposited onto a water interface. The surfactant locally lowers the surface tension in the region of deposition, and causes radial outward fluid motion along the interface. The shear stresses induced by the abrupt change in surface tension at the surfactant leading edge cause a welling up of fluid behind this disturbance. This results in the so-called “Marangoni ridge” that propagates outward from the region of deposition accompanied by a thinning of fluid behind the ridge. The induced surface flow necessarily induces subsurface flows in the bulk

fluid. Bulk flows are outward near the interface and, if the subphase is sufficiently deep for hydrostatic pressure gradients to be generated, recirculating flows develop at greater depths [36].

The mathematical theory underlying this fluid motion was accomplished in a number of papers (almost all of which occurred before 2005) that completely describe the fluid mechanics governing the Marangoni spreading on thin liquid films [36–42]. These mathematical models describe the size of the Marangoni ridge, the surface and subsurface flow fields, and the dependence of these on relevant system parameters. For a complete statement of the mathematical problem, see section 2 “Problem formulation” of reference [38]. The time-evolving positions of the contact line and Marangoni ridge have been described by power laws using scaling analyses [43–45]. This elegant and comprehensive mathematical structure has driven the research that has continued to this time.

Interfacial fluid flows could be useful in transporting therapeutics along the extensive ASL within the lung system. If the drug therapy were to contain surfactants, then the deposited solution could locally lower the ASL surface tension and induce shear stresses, which could carry the drug along the ASL and over obstructions into deeper regions of the lung. It is important to determine how this Marangoni transport can be made sufficiently long-range to access otherwise poorly medicated lung regions.

In this article, we present an overview of the work that has been done in recent years to study Marangoni transport for enhanced pulmonary drug delivery. The system in question is broadly composed of a liquid subphase and surfactant-containing drops. The manner of surfactant deposition varies in the literature and introduces key differences in process timescales. There are four main components whose time evolution will be important to understanding transport: 1) the surfactant, 2) the liquid (if there is one) in which the surfactant is carried, 3) any non-surface active species (such as drug) also carried in the liquid drop, and 4) the subphase onto which the drop is deposited.

As we proceed, it will be helpful to keep in mind the broad web of possible materials used in these systems as well as the timescales involved. The surfactant may be soluble or insoluble in the bulk subphase, the drop, or both. An insoluble surfactant, such as a phospholipid, would be carried in the drop as a dispersion of vesicles. The solvent in the drop may be miscible or immiscible with the subphase. These solubility effects will depend on the timescale of the spreading event. For example, a soluble surfactant may act as if it were insoluble, or a miscible drop may maintain an effective interfacial tension with the bulk on short timescales if the rate of spreading along the interface far exceeds the rate of transport into the bulk. The surfactant may be delivered without a fluid carrier (i.e. as a “neat” layer of surfactant), or by a surfactant-containing drop with a distinct contact line on the subphase (i.e. as a drop of solution, insoluble surfactant dispersion, or “neat” liquid surfactant). The “drug” to be delivered may be surface active or non-surface active, hydrophilic or hydrophobic. These different systems will all have different transport behaviors and optimizing these behaviors will require a thorough understanding of the variables mentioned above.

We will begin with a brief discussion of the current understanding of the role of SRTs and phospholipids in reducing the ASL surface tension and promoting airway re-opening. We will then move on to a discussion of surfactant-induced Marangoni transport on fluid subphases where the surfactant is delivered by microliter drops or by liquid aerosols. Next, we will describe the use of surfactants naturally found in the lung to induce this transport. We will end with a number of open topics for further research and discussion.

2. SRTs and phospholipids for surface tension reduction

A recent review by Grotberg and collaborators [46] discusses in detail the advancements in understanding of SRT delivery. They discuss how airways close at the end of expiration, due to low pressure within the airways as well as external pressure from decreasing chest volume, and how this closure can be a problem for those with pulmonary disease. If closure occurs early, there is likely inhomogeneous distribution of ventilation in the lung. Airway closure is usually due to liquid plugs from capillary (Rayleigh) instabilities or from the collapse of the elastic wall of the airway (capillary-elastic instability). Re-opening occurs when inspiration forces air against these liquid plugs. The air pressure moves the plugs, dragging them deep into the lung and leaving fluid on the airway surface as they move. Once enough fluid has been left on the sides of the airways, the liquid bridge becomes thin and breaks, which releases a shock of energy (heard as a crackle in sick patients lungs). SRT solutions are typically instilled directly into the patient's airways as a liquid bolus and these plugs of medication are moved down the airway tree in a similar manner, decreasing in volume as they go, and leaving SRT solution on the airway lining.

A number of groups have done extensive modeling of SRT formulation flows within the airway tree, using variables including the pressure of inhalation, the angles of branches, and the direction of gravity to predict where the bolus SRT fluid will end up [46–48], to predict the optimal air flow pattern for maximum delivery and minimum airway damage [49], and to understand the capillary mechanics of the thin fluid films within the lung [50,51]. In this way they have been able to make detailed predictions of SRT distributions within 3D models of the lung airway tree. Some groups have even suggested that bolus delivery of these SRT fluids may be inducing surface tension gradients which act to draw the SRT further into the lung and have described how the presence of pre-existing, endogenous lung surfactant may inhibit or augment the spreading rate of this motion [52,53].

Previous work shows that the components of SRT formulations in aqueous dispersion are able to generate surface tensions as much as 46 mN/m lower than that of water [18–20,54]. This work focuses on how phospholipid-containing vesicle structures within the formulations slowly break open at the surface. As will be discussed later, while these surface tensions suggest that deposited drops of phospholipid dispersions should be able to induce Marangoni transport upon deposition onto a water surface, transport is not induced in this case because the timescale for vesicle-opening is longer than the timescale for diffusion of the vesicles away from the interface [55].

3. Marangoni transport along thin fluid interfaces

Significant work has been done in the past few years, both theoretically and experimentally, to better understand the mechanics of surfactant-driven transport in systems that mimic the lung. These are systems that include thin fluid films and/or entangled mucin or other water-soluble polymer solutions that mimic mucus. Comparisons have been made for single drop versus aerosol deposition and for soluble versus insoluble surfactants. The connection between transport of surfactants and non-surface active solutes has been established.

3.1 Single source Marangoni transport

Modeling of Marangoni spreading at fluid surfaces has been developed over many years, notably in the groups of Grotberg and Matar [36,38,41,56]. This work deals primarily with a single deposited source of surfactant, either in the form of a surfactant-laden fluid drop placed on the surface where it forms a lens, or a neat layer of surfactant pre-deposited onto the surface and separated from the full surface area by a removable physical boundary. Differences between these two cases are subtle and primarily have to do with the existence or non-existence of a drop contact line. This contact line can alter fluid flow by creating a potential energy barrier to lateral fluid motion across the interface. In the case of drop deposition, where a contact line expands outward during the spreading event, the surfactant crosses the contact line, but non-surface active species tend not to do so, instead remaining within the drop area [57–60]. This means that surfactant spreads further than non-surface active solutes.

A few fundamental concepts from the earlier modeling work will be important for further discussion. In their 1990 and 1992 papers [36,38], Gaver, Grotberg, and Jensen describe the difference in the fluid dynamics of Marangoni spreading on a thin film and that on a deep pool. In the deep pool regime, the outward spreading is compensated by an inward recirculating flow below the Marangoni ridge, as dictated by mass conservation. However, in thin film regimes, the outward fluid flow profile penetrates down to the lower bounding interface, which disallows recirculation flow in the ridge and can result in de-wetting of the interface. The dimensionless parameter distinguishing these two regimes is the “gravitational parameter”, G, which describes the ratio of the gravitational driving force and the surface-tension gradient force governing the flow: $G = \rho H^2 g/S$, where ρ is the subphase density, H is the subphase depth, g is the acceleration due to gravity, and S is the difference in surface tension between the surfactant-laden region and the clean interface. When G is less than about 0.5, de-wetting is likely to occur. Larger G values will result in diminished Marangoni ridge heights, greater surfactant concentration near the center of the drop, and slower outward motion of the drop boundary as compared to smaller G values [38]. Much of the work discussed in this article will be near this critical G value.

Recently, fluid dynamic models of drops deposited on thin films have become more advanced and now incorporate a significant number of effects relevant to spreading in the lung. Matar and collaborators have developed powerful models for spreading drops that include surfactants capable of diffusion and convection at and between interfaces as well as between the drop and the subphase. In these models, the drop solvent is immiscible with the bulk, but the surfactant solubility may be specified in both phases. These are thin film

models that allow for adjustment of surfactant concentration, including micellar effects, subphase viscosity, and subphase depth. They predict the formation of the characteristic Marangoni ridge induced by the surface tension gradient along the interface (see Figure 1). The ability to model the progression of these drops with various boundary conditions and types of surfactant is essential to the prediction of how they will behave in a more complex system such as that of the ASL.

A number of groups have been experimentally examining the intricacies of these Marangoni flows induced by surfactant-containing drops (for example, see [57,61–64]). Wang and collaborators did a series of experiments using a high-speed camera to simultaneously monitor the capillary waves, Marangoni ridge, drop contact line, and tracer particle motion [65]. In these experiments, a 4 μL drop of soluble surfactant solution was deposited onto a ~ 3 mm deep, water film. The camera was used to record the early spreading behavior before the Marangoni ridge hit the edge of the experimental Petri dish. In this setup, waves on the subphase are seen as shadow bands in the images (see Figure 2). When a drop of pure water was placed on the water surface, capillary waves moved out from the point of deposition and their well-known dispersion relation was observed. Tracer particles on the water surface were not transported laterally by these capillary waves. When a drop of surfactant was placed, a larger dark band trailed the capillary waves and caused outward motion of the tracer particles as it passed them. This was assumed to be the Marangoni ridge.

This work captures a number of important features of Marangoni transport from surfactant solution drops. First, it shows that the capillary waves have the fastest propagation in the system at a velocity of 0.8 – 1.1 m/s depending on the surfactant used. Second, it shows that the Marangoni ridge follows the capillary waves and, unlike those waves, contains a lateral velocity field that is able to displace tracer particles along the interface. This circular Marangoni ridge propagates with the expected power law behavior with time for these conditions ($R \sim t^{0.7}$) [43,44,66,67]. The exact value of this power is quite sensitive to details of the experiment. Third, it shows that the contact line of the original surfactant-containing drop is quickly surpassed by the Marangoni ridge and trails the other features of spreading. Finally, it shows that even relatively small ~ 100 μm PMMA tracer beads may not be reliable indicators of the position of the Marangoni ridge, due to the fact that they trail behind the ridge after being initially moved by it. This last point is important for those wishing to study Marangoni effects. Tracing fluid flow and having accurate diagnostics for determining the location of the Marangoni ridge and contact line are essential to the understanding of these systems. Many groups use talc powder or small tracer beads to indicate fluid flow and, while these are useful measurements, the tracers should not be assumed to mark the location of the Marangoni ridge front.

In addition to being able to model the shape and dynamics of the Marangoni front, it is important to understand the differences in spreading behaviors between different types of surfactants that could be used to initiate these flows. Starov and collaborators have done significant work to understand the differences between soluble and insoluble surfactants as well as between surfactant solutions above and below their critical micelle concentration (CMC) [62,68]. They examined the early-time spreading of two surfactants, sodium dodecyl sulfate (SDS) and dodecyltrimethylammonium bromide (DTAB) on water. At early times,

SDS is treated as an insoluble surfactant due to its low rate of desorption from the surface into the subphase; DTAB has a faster desorption rate in water due to its much higher solubility and, thus, behaves as a soluble surfactant during early spreading. Droplets of solutions of each surfactant were deposited onto water and the resulting spreading was observed with a high-speed camera and compared to the theoretically predicted power-law behavior of drop radius with time. As with many spreading phenomena here, time scales play a crucial role through the dependence of the apparent solubility of the surfactant on the timescale of the experiment.

For droplets of surfactant solution above the CMC deposited onto water, spreading occurs in two stages: first a faster power law spreading ($R \sim t^{0.5}$) as micelles disintegrate, and second a slower power law spreading once there is no longer a micelle reservoir [62]. Below the CMC, spreading also occurs in two stages: first, a much shorter fast-spreading stage and second, a longer slow-spreading stage. During the first stage, the spreading power law exponent is consistently approximately 0.5, independent of solubility. However in the second stage in either case, the spreading power law depends heavily on whether the surfactant is soluble or insoluble. In the case of insoluble surfactants (SDS in their case), the total surfactant mass at the interface does not change and the power law in the second stage is predicted to be 0.25 (observed to be 0.21). In the case of soluble surfactants (DTAB in their case), the total surfactant mass at the interface decreases as the surfactant desorbs into the bulk, therefore the spreading exponent is significantly smaller, around 0.03 for DTAB.

These subtle differences between surfactants with different characteristics could have important implications in the lung. If their in vivo spreading behavior follows Starov's prediction, insoluble surfactants will produce greater total spread areas than soluble surfactants. However, with repeated deposition, they could also eventually saturate the surface and perhaps terminate spreading or cause physiological difficulties in eventual surfactant removal from the surface. Conversely, while soluble surfactants may desorb from the surface and generate a lower spread area per deposition, this may also make repeated dosings more effective once the surface returns to a higher surface tension.

3.2 Multiple source Marangoni transport

All of the work discussed thus far has been related to drop-wise deposition of surfactant onto a water subphase. Yet, aerosolization is one of the primary methods by which therapeutics are delivered into the lung. There are two primary differences between delivery via microliter (macroscopic) drops and via picoliter (microscopic) aerosol droplets. First, the comparative drop lengthscales will dictate the relative timescales for diffusion with the subphase and convection along the surface. Second, operationally, the aerosol will be deposited as a field of droplets over a sustained administration, which will introduce several timescales as discussed below.

Khanal and Sharma published a pair of articles comparing rates of aerosol delivery to a fluid subphase [69,70]. They suggest four important timescales for surfactant delivery and spreading. $\tau_{monolayer}$ is the time it takes to deliver a complete monolayer of droplets onto the area of interest, $\tau_{spreading}$ is the time it takes for an individual droplet to complete convective spreading after deposition, $\tau_{lateral}$ is the timescale for lateral motion of the centroid of a

single drop due to the Marangoni forces exerted by neighboring drops, and $\tau_{coalescence}$ is the timescale for coalescence of neighboring drops. The interplay between these various timescales will control the dynamics of the cumulative Marangoni transport caused by multisource aerosol deposition.

This pair of articles focuses on controlling $\tau_{monolayer}$ and describes two regimes of aerosol flux. At high aerosol fluxes, when $\tau_{monolayer}$ is small compared to $\tau_{spreading}$ and $\tau_{lateral}$, the aerosol droplets combine on the surface and propagate outward as a single, parabolic front (shown in Figure 3D and discussed in [69]). In this case, the aerosol droplet solvent plays a more important role and the whole field of droplets acts like one large drop. At lower fluxes, when $\tau_{monolayer}$ is large compared to $\tau_{spreading}$ and $\tau_{lateral}$, distinct aerosol droplets can be seen landing and spreading on the interface and then propagating outward as an expanding field of distinct spots (shown in Figure 3B and discussed in [70]). The individual deposited droplets also appear to repel each other and do not coalesce. In this low-flux regime, the solvent has time to diffuse into the bulk before more aerosol is deposited, so the surfactant acts more like a "neat" layer of surfactant. Here, although the individual aerosol droplets do spread on their own, it is the surface tension gradient from inside the field to outside the field that drives the dispersal of aerosol contents along the surface.

High and low flux deposition have physiological implications when considering the bifurcating branch network of the lung airways. Different airway generations will experience different aerosol deposition fluxes impacting on the ASL. Using the Wiebel model of the lung [4], clinically relevant dosage rates, and models for inertial deposition for aerosols of known diameter and density, Khanal and Sharma predicted the deposition flux for aerosols in different lung generations. The predicted deposition fluxes in the large airways (generations ~ 1 – 8) of approximately 0.02 to 0.12 $\mu L/cm^2 \bullet sec$ matched their conditions of the high flux experiments, while predicted fluxes in the lower airway (generations > 8) of well below 0.01 $\mu L/cm^2 \bullet sec$ matched those of the low flux experiments. Thus, depending on inspiration flows and aerosol dosages, the upper airways are likely to experience drop-like spreading of pooled aerosol droplets drug while the lower airways should experience drug delivery via post-deposition dispersal of droplet fields. In both flux regimes, Marangoni transport dispersed aerosol contents over anatomically significant areas, corresponding to at least one full airway generation.

4. Use of phospholipids and SRTs for Marangoni transport in the lung

4.1 Seeking biocompatibility: phospholipids

The ultimate goal in this review is to convey the potential for Marangoni spreading as an enhanced drug dispersion mechanism on the ASL. To this end, it is useful to discuss the ability of the lung's own natural surfactants to induce transport. The lung produces phospholipids and surfactant-associated proteins that function to reduce the surface tension within the alveoli. If we propose to add surfactants to inhaled medications to induce Marangoni spreading, such natural surfactants would likely be safer for human use than synthetic surfactants. The most abundant surface tension lowering agent in lung surfactant is the phospholipid dipalmitoylphosphatidylcholine (DPPC) [9]. Phospholipids are amphiphilic molecules consisting of a hydrophilic head group and two hydrophobic, aliphatic carbon

tails. Thus, they are extremely insoluble in water (with a solubility of ~ 10^{-8} M [71]) and have a strong affinity for air-water interfaces. There is a large body of work, mostly in the form of Langmuir trough measurements of lipid monolayer surface pressure-area isotherms and their interpretation in terms of monolayer phase behavior, showing that phospholipids at air-water interfaces lower the interfacial tension significantly (For examples, see [72–79]).

4.2 Phospholipids transport from a "neat", confined region

Neat phospholipid deposits have been shown to induce Marangoni transport when placed directly onto a confined region of a glycerol surface and then released from that confined region to spread outward [80,81]. In this set of articles by Daniels and collaborators, DPPC was dissolved in chloroform and deposited directly onto a ~ 1 mm thick glycerol film within a confinement ring. The chloroform was allowed to evaporate and then the ring was gently lifted to allow the lipid to spread across the full area of the interface. The first article of the pair used a laser light sheet and fluorescently modified lipid in order to simultaneously track Marangoni ridge height and lipid concentration as a function of radial distance from the deposition center [80]. The laser light sheet was deformed linearly by changes in fluid height and the intensity of fluorescence at any given position determined the surfactant concentration at that point.

In the second article [81], the experiments from [80] were used to confirm that the Marangoni ridge profile closely resembled that predicted in earlier theory papers by Gaver and Grotberg [36], which described the release of insoluble "neat" surfactant from a confined surface region. However, the concentration profiles observed had significant discrepancies from theoretical predictions. Theory predicts a smooth, monotonic decrease in surfactant concentration from the deposition region outward, but Daniels and collaborators saw a smooth decrease to a plateau, and then a sharp decrease near the peak of the Marangoni ridge (see Figure 4). This deviation from theory is likely due to a lack of understanding of the dynamic roles played by lipid phase transitions and the varying compressibility of the layer as a function of surface concentration in an expanding lipid monolayer. Within lipid monolayers at interfaces, there can be long-range associations between molecules. This means that, upon release, the molecules may not homogeneously spread outward to cover the new open space, but may go through surface phase transitions and phase coexistence regions that will depend on the makeup and temperature of the system [82–84].

4.3 Phospholipids transport through aerosolization

Although phospholipids are promising candidates for inducing transport over the ASL based on anticipated safety, the problem of how to get the surface-active lipid to the ASL surface at a rate and surface concentration sufficient to drive Marangoni transport is non-trivial. When lipids are dispersed in an aqueous medium, their low solubility results in the immediate formation of lipid vesicles – where all of the hydrophobic tail groups are sequestered within bilayers. The lipid headgroups exposed at the surface of these vesicles are hydrophilic and, thus, the vesicle structure itself is not surface active. Although the vesicle dispersion may achieve a lower surface tension than water at long times due to the relatively slow process of

vesicle diffusion and breakup at the air/water interface [85,86], drops of phospholipid vesicle dispersions do not initiate Marangoni transport when placed on a clean water interface [55].

One way to liberate lipid molecules from within vesicles in order to rapidly establish a monolayer at the air/water interface is through aerosolization [87–89]. As shown by Stetten and collaborators, aerosolizing a lipid dispersion directly onto a fluid interface activates the dispersion to initiate Marangoni transport [55]. This aerosolization process is highly energetic – it acts to shear open the lipid vesicles, store lipids as adsorbed monolayers on the surfaces of the resulting aerosol droplets, and transfer that monolayer directly to a fluid interface upon deposition. This work has shown that aerosolized lipid dispersions can transport tracer particles over many centimeters of interface and lower the subphase surface tension to values less than 10 mN/m (see Figure 5C).

This phospholipid-induced Marangoni transport has been observed on water as well as on a 5% porcine gastric mucin (PGM) solution consisting of high-molecular weight mucins to mimic ASL (see Figure 5A) [90]. These solutions have initial surface tensions significantly lower than that of water (~ 34 mN/m), yet this does not hinder transport. Additionally, further work of Iasella and collaborators has shown that aerosolized phospholipid-induced Marangoni transport occurs even in the presence of a pre-deposited, dense monolayer of DPPC on the mucin solution surface (see Figure 5B). Considering the likelihood that a layer of phospholipid exists atop the ASL within certain regions of the lung airways, and that the density of these monolayers likely varies significantly with respect to airway generation and physiological conditions, this finding is quite significant. It indicates that pre-existing pulmonary surfactant would not likely suppress Marangoni transport of aerosolized therapies.

Whenever Marangoni transport is initiated at a fluid interface, the tangential surface stress drives subsurface fluid flow. This induced subsurface flow has been observed experimentally by many groups including in the case of phospholipid-induced transport above (see Figure 6) [55]. The subsurface flow may be critical to the transport of non-surface-active drug species. Many antibiotics currently used in the treatment of chronic lung infection are hydrophilic (such as the commonly used antibiotic, tobramycin). Upon droplet deposition, such water-soluble drugs would remain in the aqueous phase just beneath the surface. Entrainment in the sub-surface flow will produce the intended post-deposition dispersal.

Iasella and collaborators have shown that subsurface flows induced by phospholipid Marangoni transport are sufficient to carry the antibiotic tobramycin outward from the region of aerosol deposition on mucin solution subphases with pre-deposited lipid monolayers (see Figure 6) [90]. When tobramycin was added to the aerosolized phospholipid dispersions at clinically appropriate concentrations, antibiotic concentrations of over 8 μg/mL were found across the PGM solution surface as far as 8.5 cm away from the region of deposition. For reference, the minimum inhibitory concentration (MIC90) of tobramycin for *Pseudomonas aeruginosa*, a common CF-associated pathogen, is 8 μg/mL [28].

The strength of the Marangoni transport driving force, and its persistence over large areas of surfactant spreading, depend critically on the surface pressure-area isotherm of the lipid. In this work transporting aerosolized lipid against a pre-deposited lipid layer, the authors also created lipid surface pressure-area isotherms on both water and mucin. Mucin solutions have a significantly lower surface tension than water due to adsorption of hydrophobic moieties to the interface. It was found that, although the isotherms are significantly different for most monolayer densities, they converge at high lipid densities. Monolayer collapse surface tensions for monolayers on water or on aqueous PGM solutions were nearly identical. This suggests that the final state just prior to collapse in both cases is a pure lipid monolayer, rather than a mixed monolayer of lipid and mucins on the mucin solution. This agrees with previous work stating that amphiphilic water-soluble polymers are able to adsorb into expanded lipid monolayers but are excluded from lipid monolayers as they are compressed into the liquid condensed state [91,92].

Work involving phospholipid-induced Marangoni transport has an interesting connection to the work involving use of SRT formulations to treat RDS. All currently approved SRT formulations comprise animal-derived lung surfactant and are delivered as an instilled bolus. Because they contain phospholipids as a major component, it is possible that aerosolization of SRT solutions into the lungs, instead of delivery via bolus instillation, might open up lipid vesicles and induce surface flow in the same way as do dispersions of pure phospholipid [93,94], thus improving distribution. Lewis and collaborators directly examined the physiological differences between SRT formulation delivery via bolus and via aerosol to treat lung injury in adult rabbits [93]. The test subjects were given 1) nebulized beractant (a common SRT formulation), 2) nebulized saline, 3) pure carrier gas, or 4) tracheally instilled beractant. The ventilation efficiency index increased over 3 hours with nebulized beractant, but decreased in the other three cases. Additionally, the group given nebulized beractant was the only group to experience increased lung compliance during the trial and also had significantly greater lung volume at maximum pressure. These positive signs for improved lung function were achieved only when the SRT formulation was aerosolized. This was true despite the delivery of much greater total amounts of SRT formulation in the case of tracheal instillation (100 mg/kg) than aerosolized administration (5 mg/kg).

There are, of course, many factors that could have led to increased efficacy of SRT delivery via aerosolization over instillation. However, one possibility is that the aerosolized SRT formulations led to more complete and homogeneous delivery due to induced Marangoni transport. Previous work by Marcinkowski and collaborators has shown that when the SRT agent Calfactant is aerosolized onto cultured human bronchial epithelial cell monolayer from a CF patient, the resulting deposition area is greater than when pure saline is aerosolized onto the surface [95]. This suggests that SRT formulations can and do induce Marangoni transport when aerosolized onto model biological surfaces. It is difficult, however, to directly compare spreading on these cultured bronchial epithelial cells to what might occur within the lung itself. The lung is a complex system containing numerous regions with likely different surface chemistries. The surface tension in any given region (and any given patient) remains an important open question in this field.

5. Conclusions and Open Questions

Recent work has produced significant advancements in the understanding of Marangoni transport for potential use in complex systems such as that of the human lung. These advancements would not have been possible without innovative, collaborative research from a number of different fields. Complex fluid dynamics models predict how fluid transport occurs on thin fluid films and reveal effects from a multitude of important variables such as fluid depth, boundary conditions, viscosity, and surfactant solubility. Experimental work has tested these models and begun to reveal the differences between surfactant delivery by individual microliter drops and multiple depositing picoliter aerosol droplets. New ways of delivering phospholipid surfactants to the subphase surface have been explored and aerosolization has been shown to release surface-active lipids from vesicles so they may induce Marangoni transport. This work has furthered our understanding of how Marangoni transport might be used to increase the effectiveness of pulmonary drug delivery, still there are significant open questions yet to be answered. We will outline a few of these topics here.

As addressed in the previous section, one of the major open questions has to do with the functionality of SRT formulations. If these therapeutics result in better physiological outcomes when delivered via aerosol, it could be possible that aerosolization is activating the phospholipid constituents and causing Marangoni transport. The mechanism by which aerosolization disrupts vesicles and aids in the transfer of lipids to the air/water interface has yet to be determined. Preliminary work by one of the authors (Stetten) has shown that Infasurf SRT does not induce Marangoni transport on porcine gastric mucin when deposited as a microliter drop, but does induce transport when aerosolized, suggesting a similar initiation mechanism as occurred with pure phospholipid dispersions. However, these experiments were conducted far below body temperature (24 C), so it could be the case that, at body temperature (37 C), peptide components of the SRTs act to destabilize lipid vesicles and promote opening of these vesicles at the interface. It is known that the combination of phospholipid and peptides in lung surfactant increase the stability of monolayers allowing for the achievement of very low surface tensions in the alveoli (described in many references, including [17,96–99]). If the roles and physical states of these various components during aerosolization were better understood, then one could isolate and optimize the “active ingredients” necessary for Marangoni transport and surface tension reduction.

A second interesting topic for further investigation is the competition of phenomena with different timescales during drug delivery. Aerosol delivery, intermixing of drop and subphase contents, and mucociliary clearance interact and compete in complex ways within the lung. The velocity of Marangoni transport, and additionally the height of the Marangoni ridge, depends on the surface tension gradient along the interface. One might expect that maintenance of the largest gradient possible would result in the best outcome. However, the mucosal fluid plus the PCL is only microns thick in many places and the airways themselves can be as small as a few hundred microns in diameter. This means that the Marangoni ridge could cause bridging of fluid across the airway or the trailing fluid depression could cause de-wetting of the PCL or underlying cells [100–103]. Optimization of the delivery and spreading timescales to maximize spread area of the drug while avoiding potentially

catastrophic de-wetting is a critical question in this work. It is feasible that we have a "tortoise and the hare" problem – that the optimal surface tension gradient may be one that is smaller, but is maintained for a longer time to achieve the same result (without being so slow that mucociliary clearance negates the effects). If the optimization point between competing rates could be predicted, spreading results could be better controlled.

In addition to timescale considerations, we must also consider the varying length scales in pulmonary delivery. Since the ASL is quite thin, it is possible that the subsurface flows observed on deeper pools may not be as capable of transporting drug on these thinner films. When phospholipids are aerosolized onto water, excess lipid re-aggregates beneath the surface to form 10 μm diameter structures. Clearly these structures would have an effect on transport in a 10 μm thick film. Flow in such thin films in the lung is not perfectly captured by models such as that discussed by Matar due to the fact that the mucosal fluid layer in the lung resides atop a second layer, the cilia-containing PCL. In order to fully understand any possible de-wetting phenomena as well as subsurface flow within the lung, the ASL has begun to be modeled as a two-layer system: a viscous complex fluid (the mucus layer) atop a porous medium (the PCL) [7]. In this two-layer system, the lower boundary condition on the spreading subphase changes from a no-slip condition to a tangential stress-matching condition, altering spreading rates and allowing for the possibility of re-wetting through fluid flow up out of the porous medium.

Another open question is that of solubility in these systems. This can come in a number of forms: 1) miscibility of the drop solvent in the bulk, 2) solubility of the surfactant in either the drop or bulk, and 3) solubility of the drug in either the drop or bulk phase. The question of miscibility of the drop solvent is really another timescale system. Since even miscible fluids maintain an effective interfacial tension as they dissolve into a subphase, the timescale over which this interface is maintained becomes important to understanding the capillary behavior of the drops. As discussed above, the solubility of the surfactant can lead to differences in the rate of spreading as well as differences in the final state of the system. The solubility of the drug will dictate how that drug would best be delivered into the system (i.e. within a lipid vesicle [104], solubilized in micelles, or molecularly dissolved within the aqueous phase, etc.). Additionally, if the drug were surfactant-like, it is possible that it could initiate Marangoni transport without the need for additional transport enhancers. This might be especially useful when spreading over thin films with little subsurface volume.

The final piece to this puzzle is, unfortunately, one of the most difficult to attain. There is widespread disagreement on the surface tension of the lung ASL, and there is no doubt that it must vary with respect to location in the lungs. As mentioned earlier, many groups have tried different experimental methods to determine ASL surface tensions, but the range of surface tensions reported is extremely large, ranging from 5 to 90 mN/m [10–15]. This is due to the physical difficulty of taking a measurement within a live subject. In order to fully model transport within this system, it is crucial that we have a better understanding of the ASL surface tension and its homogeneity. In the engineering sense, drug delivery formulations must be designed with sufficient margin of error to drive Marangoni transport against low surface tensions. The observed transport driven by aerosolized phospholipids against densely packed DPPC monolayers suggests this is feasible.

These open questions show that there is ample opportunity for further exciting, interdisciplinary study, of both fundamental and applied nature, with promising potential clinical impact. There are many opportunities to extend the current knowledge of wetting and spreading phenomena to address the unique compositional, rheological and surface chemical complexities afforded by the lung system.

Acknowledgments

We would like to acknowledge graduate student Madeline Salueda for thoughtful discussions and suggestions. This work was funded in part by the National Science Foundation under grants CBET-1510293 and in part by the National Heart, Lung and Blood Institute of the National Institutes of Health under grant R01 HL 105470.

Bibliography

1☆. Bansil R, Turner BS. Mucin structure, aggregation, physiological functions and biomedical applications. Current Opinion in Colloid & Interface Science. 2006; 11:164–170. A review of mucin structure and physiological function. DOI: 10.1016/j.cocis.2005.11.001

2. Samet JM, Cheng PW. The Role of Airway Mucus in Pulmonary Toxicology. Environ Health Perspect. 1994; 102:89–103.

3. Veldhuizen R, Nag K, Orgeig S, Possmayer F. The role of lipids in pulmonary surfactant. Biochimica Et Biophysica Acta. 1408(1998):90–108. DOI: 10.1016/S0925-4439(98)00061-1

4. Weibel ER, Gomez DM. Architecture of the human lung. Use of quantitative methods establishes fundamental relations between size and number of lung structures. Science. 1962; 137:577–585. [PubMed: 14005590]

5. Lee PS, Gerrity TR, Hass FJ, Lourenco RV. Model for Tracheobronchial Clearance of Inhaled Particles in Man and a Comparison with Data. Ieee Transactions on Biomedical Engineering. 1979; 26:624–630. DOI: 10.1109/TBME.1979.326544 [PubMed: 511197]

6. Lillehoj EP, Kato K, Lu W, Kim KC. Chapter Four – Cellular and Molecular Biology of Airway Mucins. Elsevier; 2013.

7☆☆. Button B, Cai L-H, Ehre C, Kesimer M, Hill DB, Sheehan JK, et al. A periciliary brush promotes the lung health by separating the mucus layer from airway epithelia. Science. 2012; 337:937–941. An article which probes the properties of the PCL and begins to understand it as a porous media rather than a Newtonian fluid. DOI: 10.1126/science.1223012 [PubMed: 22923574]

8. Cai L. doctoral dissertation. 2012. Structure and function of airway surface layer of the human lungs & mobility of probe particles in complex fluids.

9. Poulain FR, Clements JA. Pulmonary Surfactant Therapy. Western J Med. 2014:1–8.

10. Albers GM, Tomkiewicz RP, May MK, Ramirez OE, Rubin BK. Ring distraction technique for measuring surface tension of sputum: Relationship to sputum clearability. Journal of Applied Physiology. 1996; 81:2690–2695. [PubMed: 9018523]

11. Brown ES, Johnson RP, Clements JA. Pulmonary Surface Tension. Journal of Applied Physiology. 1959; 14:717–720. [PubMed: 13804921]

12. Clements JA, Brown ES, Johnson RP. Pulmonary Surface Tension and the Mucus Lining of the Lungs: Some Theoretical Considerations. Journal of Applied Physiology. 1958; 12:262–268. [PubMed: 13525272]

13. Hills BA. Alveolar Liquid Lining - Langmuir Method Used to Measure Surface -Tension in Bovine and Canine Lung Extracts. J Physiol (Lond). 1985; 359:65–79. [PubMed: 3839017]

14. Schürch S, Goerke J, Clements JA. Direct determination of surface tension in the lung. Proc Natl Acad Sci USa. 1976; 73:4698–4702. [PubMed: 1070020]

15. Schürch S, Goerke J, Clements JA. Direct determination of volume- and time-dependence of alveolar surface tension in excised lungs. Proc Natl Acad Sci USa. 1978; 75:3417–3421. [PubMed: 277943]

16. Shier D, Butler J, Lewis R. Hole's Human Anatomy and Physiology. 11. McGraw Hill; 2007.

17☆. Ding J, Takamoto DY, von Nahmen A, Lipp MM, Lee KYC, Waring AJ, Zasadzinski JA. Effects of Lung Surfactant Proteins, SP-B and SP-C, and Palmitic Acid on Monolayer Stability. Biophysical Journal. 2001; 80:2262–2272. An article which experimentally observes the effects of lung proteins on the stability of lipid monolayers. DOI: 10.1016/S0006-3495(01)76198-X [PubMed: 11325728]

18. Kim SH, Park Y, Matalon S, Franses EI. Effect of buffer composition and preparation protocol on the dispersion stability and interfacial behavior of aqueous DPPC dispersions. Colloids and Surfaces B: Biointerfaces. 2008; 67:253–260. DOI: 10.1016/j.colsurfb.2008.09.003 [PubMed: 18930639]

19. Kim SH, Haimovich-Caspi L, Omer L, Talmon Y, Franses EI. Effect of sonication and freezing-thawing on the aggregate size and dynamic surface tension of aqueous DPPC dispersions. Journal of Colloid and Interface Science. 2007; 311:217–227. DOI: 10.1016/j.jcis.2007.02.060 [PubMed: 17359989]

20☆. Kim SH, Franses EI. New protocols for preparing dipalmitoylphosphatidylcholine dispersions and controlling surface tension and competitive adsorption with albumin at the air/aqueous interface. Colloids and Surfaces B: Biointerfaces. 2005; 43:256–266. An article which experimentally observes the gradual reduction in surface tension of lipid dispersions as vesicles break open at the interface. DOI: 10.1016/j.colsurfb.2005.05.006 [PubMed: 15979858]

21. Kirkness JP, Eastwood PR, Szollosi I, Platt PR, Wheatley JR, Amis TC, et al. Effect of surface tension of mucosal lining liquid on upper airway mechanics in anesthetized humans. Journal of Applied Physiology. 2003; 95:357–363. DOI: 10.1152/japplphysiol.01198.2002 [PubMed: 12626492]

22. Newman SP, Agnew JE, Pavia D, Clarke SW. Inhaled aerosols: lung deposition and clinical applications. Clin Phys Physiol Meas. 1982; 3:1–20. DOI: 10.1088/0143-0815/3/1/001 [PubMed: 7049509]

23. Anzueto A, Baughman RP, Guntupalli KK, Weg JG, Wiedemann HP, Raventós AA, Lemaire F, Long W, Zaccardelli DS, Pattishall EN. Aerosolized Surfactant in Adults with Sepsis-Induced Acute Respiratory Distress Syndrome. 2009; 334:1417–1422. Http://Dx.Doi.org/10.1056/NEJM199605303342201. DOI: 10.1056/NEJM199605303342201

24. Hattrup CL, Gendler SJ. Structure and Function of the Cell Surface (Tethered) Mucins. Annu Rev Physiol. 2008; 70:431–457. DOI: 10.1146/annurev.physiol.70.113006.100659 [PubMed: 17850209]

25. Brown JS, Zeman KL, Bennett WD. Regional deposition of coarse particles and ventilation distribution in healthy subjects and patients with cystic fibrosis. Journal of Aerosol Medicine. 2001; 14:443–454. DOI: 10.1089/08942680152744659 [PubMed: 11791685]

26. Fiel SB. Aerosolized antibiotics in cystic fibrosis: an update. Expert Rev Respir Med. 2014; 8:305–314. DOI: 10.1586/17476348.2014.896205 [PubMed: 24838090]

27. Restrepo MI, Keyt H, Reyes LF. Aerosolized Antibiotics. Respiratory Care. 2015; 60:762–773. DOI: 10.4187/respcare.04208 [PubMed: 26070573]

28. Shawar RM, MacLeod DL, Garber RL, Burns JL, Stapp JR, Clausen CR, Tanaka SK. Activities of tobramycin and six other antibiotics against Pseudomonas aeruginosa isolates from patients with cystic fibrosis. Antimicrobial Agents and Chemotherapy. 1999; 43:2877–2880. [PubMed: 10582875]

29. Strateva T, Petrova G, Mitov I. Antimicrobial activity of tobramycin against respiratory cystic fibrosis Pseudomonas aeruginosa isolates from Bulgaria. J Chemother. 2010; 22:378–383. DOI: 10.1179/joc.2010.22.6.378 [PubMed: 21303744]

30. Sexauer WP, Fiel SB. Aerosolized antibiotics in cystic fibrosis. Semin Respir Crit Care Med. 2003; 24:717–726. DOI: 10.1055/s-2004-815667 [PubMed: 16088587]

31. Svartengren K, Lindestad P-Å, Svartengren M, Bylin G, Philipson K, Camner P. Deposition of inhaled particles in the mouth and throat of asthmatic subjects. Eur Respir J. 1994; 7:1467–1473. DOI: 10.1183/09031936.94.07081467 [PubMed: 7957832]

32. Merlo CA, Boyle MP, Diener-West M, Marshall BC, Goss CH, Lechtzin N. Incidence and risk factors for multiple antibiotic-resistant Pseudomonas aeruginosa in cystic fibrosis. Chest. 2007; 132:562–568. DOI: 10.1378/chest.06-2888 [PubMed: 17646236]

33☆. Grotberg JB. Respiratory fluid mechanics and transport processes. Annu Rev Biomed Eng. 2001; 3:421–457. A review of a variety of biomechanical fluid processes in the lung. DOI: 10.1146/annurev.bioeng.3.1.421 [PubMed: 11447070]

34☆. Bertram CD, Gaver DP. Biofluid Mechanics of the Pulmonary System. 2005; 33:1681–1688. An article which provides an overview of biofluid mechanics in the lung airways.

35. Halpern D, Jensen OE, Grotberg JB. A theoretical study of surfactant and liquid delivery into the lung. J App Physiology. 1998; 85:333–352.

36. Gaver DP, Grotberg JB. Droplet Spreading on a Thin Viscous Film. J Fluid Mech. 1992; 235:399–414. DOI: 10.1017/S0022112092001162

37. Grotberg JB, Gaver DP. A synopsis of surfactant spreading research. Journal of Colloid and Interface Science. 1996; 178:377–378. DOI: 10.1006/jcis.1996.0130

38☆☆. Gaver DP, Grotberg JB. The dynamics of a localized surfactant on a thin film. J Fluid Mech. 1990; 213:127–148. One of the key papers on Marangoni spreading on thin films. DOI: 10.1017/S0022112090002257

39☆. Afsar-Siddiqui AB, Luckham PF, Matar OK. The spreading of surfactant solutions on thin liquid films. Advances in Colloid and Interface Science. 2003; 106:183–236. A review of the fundamentals of Marangoni transport on thin films in a variety of systems. DOI: 10.1016/S0001-8686(03)00111-8 [PubMed: 14672848]

40☆☆. Karapetsas G, Craster RV, Matar OK. Surfactant-driven dynamics of liquid lenses. Phys Fluids. 2011; 23 An article which contains state-of-the-art computer modeling of Marangoni transport on thin fluid subphases. doi: 10.1063/1.3670009

41☆☆. Matar OK, Craster RV. Dynamics of surfactant assisted spreading. Soft Matter. 2009; 5:3801–3809. A concise review of important topics in surfactant-driven spreading. DOI: 10.1039/b908719m

42. De Gennes PG. Wetting: statics and dynamics. Rev Mod Phys. 1985; 57:828–861.

43. Foda M, Cox RG. The Spreading of Thin Liquid-Films on a Water-Air Interface. J Fluid Mech. 1980; 101:33–51. DOI: 10.1017/S0022112080001516

44. Joos P, Pintens J. Spreading Kinetics of Liquids on Liquids. Journal of Colloid and Interface Science. 1977; 60:507–513. DOI: 10.1016/0021-9797(77)90315-0

45. Hoult DP. Oil Spreading on the Sea. Annu Rev Fluid Mech. 1972:1–28.

46☆☆. Levy R, Hill DB, Forest MG, Grotberg JB. Pulmonary Fluid Flow Challenges for Experimental and Mathematical Modeling. Integr Comp Biol. 2014; 54:985–1000. An review which provides a description of experimental and modeling work involving pressure-driven delivery of SRTs into the lung. DOI: 10.1093/icb/icu107 [PubMed: 25096289]

47☆. Filoche M, Tai C-F, Grotberg JB. Three-dimensional model of surfactant replacement therapy. Proc Natl Acad Sci USa. 2015; 112:9287–9292. An article which describes a complex, 3D model of pressure-driven fluid motion in the lung. DOI: 10.1073/pnas.1504025112 [PubMed: 26170310]

48☆☆. Zhang YL, Matar OK, Craster RV. A theoretical study of chemical delivery within the lung using exogenous surfactant. Medical Engineering & Physics. 2003; 25:115–132. An article providing a theoretical description of chemical delivery in the lung. DOI: 10.1016/S1350-4533(02)00190-X [PubMed: 12538066]

49. Glindmeyer HW, Smith BJ, Gaver DP. In situ enhancement of pulmonary surfactant function using temporary flow reversal. J Appl Physiol. 2012; 112:149–158. DOI: 10.1152/japplphysiol.00643.2011 [PubMed: 21998268]

50. Kuchin IV, Matar OK, Craster RV, Starov VM. Influence of the Disjoining Pressure on the Equilibrium Interfacial Profile in Transition Zone Between a Thin Film and a Capillary Meniscus. ColCom. 2014; 1:18–22. DOI: 10.1016/j.colcom.2014.06.002

51. Kuchin IV, Matar OK, Craster RV, Starov VM. Modeling the effect of surface forces on the equilibrium liquid profile of a capillary meniscus. Soft Matter. 2014; 10:6024–6037. DOI: 10.1039/C4SM01018C [PubMed: 24998938]

52. Espinosa FF, Shapiro AH, Fredberg JJ, Kamm RD. Spreading of exogenous surfactant in an airway. Journal of Applied Physiology. 1993; 75:2028–2039. http://eutils.ncbi.nlm.nih.gov/entrez/eutils/elink.fcgi?dbfrom=pubmed&id=8307856&retmode=ref&cmd=prlinks. [PubMed: 8307856]

53. Grotberg JB, Halpern D, Jensen OE. Interaction of Exogenous and Endogenous Surfactant: Spreading-Rate Effects. Journal of Applied Physiology. 1995; 78:750–756. [PubMed: 7759450]

54. Wen X, Franses EI. Role of subsurface particulates on the dynamic adsorption of dipalmitoylphosphatidylcholine at the air/water interface. Langmuir. 2001; 17:3194–3201. DOI: 10.1021/la001502t

55☆☆. Stetten AZ, Moraca G, Corcoran TE, Tristram-Nagle S, Garoff S, Przybycien TM, et al. Enabling Marangoni flow at air-liquid interfaces through deposition of aerosolized lipid dispersions. 2016; 484:270–278. An article which utilizes aerosolization as a mechanism to activate lipid dispersions to initiate Marangoni transport. DOI: 10.1016/j.jcis.2016.08.076

56. Matar OK, Craster RV, Sefiane K. Dynamic spreading of droplets containing nanoparticles. Phys Rev E. 2007; 76:197–9. DOI: 10.1103/PhysRevE.76.056315

57. Sharma R, Kalita R, Swanson ER, Corcoran TE, Garoff S, Przybycien TM, Tilton RD. Autophobing on Liquid Subphases Driven by the Interfacial Transport of Amphiphilic Molecules. Langmuir. 2012; 28:15212–15221. DOI: 10.1021/la303639w [PubMed: 23039250]

58. Qu D, Suter R, Garoff S. Surfactant Self-Assemblies Controlling Spontaneous Dewetting. Langmuir. 2002; 18:1649–1654. DOI: 10.1021/la011237r

59. Kumar N, Varanasi K, Tilton RD, Garoff S. Surfactant Self-Assembly ahead of the Contact Line on a Hydrophobic Surface and Its Implications for Wetting. Langmuir. 2003; 19:5366–5373. DOI: 10.1021/la034077n

60. Starov VM. Spontaneous rise of surfactant solutions into vertical hydrophobic capillaries. Journal of Colloid and Interface Science. 2004; 270:180–186. DOI: 10.1016/j.jcis.2003.11.018 [PubMed: 14693150]

61. Koch K, Dew B, Corcoran TE, Przybycien TM, Tilton RD, Garoff S. Surface Tension Gradient Driven Spreading on Aqueous Mucin Solutions: A Possible Route to Enhanced Pulmonary Drug Delivery. Mol Pharmaceutics. 2011; 8:387–394. DOI: 10.1021/mp1002448

62☆☆. Lee KS, Starov VM. Spreading of surfactant solutions over thin aqueous layers at low concentrations: Influence of solubility. Journal of Colloid and Interface Science. 2009; 329:361–365. An article which describes the effect of surfactant solubility on the radial spreading power law exponent. DOI: 10.1016/j.jcis.2008.10.031 [PubMed: 18973905]

63. Sharma R, Kalita R, Swanson ER, Corcoran TE, Garoff S, Przybycien TM, et al. Autophobing on Liquid Subphases Driven by the Interfacial Transport of Amphiphilic Molecules. 2012; 28:15212–15221.

64. Sharma R, Corcoran TE, Garoff S, Przybycien TM, Swanson ER, Tilton RD. Quasi-Immiscible Spreading of Aqueous Surfactant Solutions on Entangled Aqueous Polymer Solution Subphases. ACS Appl Mater Interfaces. 2013; 5:5542–5549. DOI: 10.1021/am400762q [PubMed: 23705869]

65☆☆. Wang X, Bonaccurso E, Venzmer J, Garoff S. Deposition of drops containing surfactants on liquid pools: Movement of the contact line. Marangoni ridge, capillary waves and interfacial particles. 2015; 486:53–59. An article which utilizes high-speed imaging to track capillary waves, Marangoni ridge, tracer particles, and contact line after deposition of a surfactant-containing drop on a subphase. DOI: 10.1016/j.colsurfa.2015.09.029

66. Jensen OE, Grotberg JB. Insoluble Surfactant Spreading on a Thin Viscous Film - Shock Evolution and Film Rupture. J Fluid Mech. 1992; 240:259–288. DOI: 10.1017/S0022112092000090

67. Jensen OE. The Spreading of Insoluble Surfactant at the Free-Surface of a Deep Fluid Layer. J Fluid Mech. 1995; 293:349–378. DOI: 10.1017/S0022112095001741

68. Starov V, de Ryck A, Velarde M. On the Spreading of an Insoluble Surfactant over a Thin Viscous Liquid Layer. Journal of Colloid and Interface Science. 1997; 190:104–113. [PubMed: 9241147]

69☆☆. Khanal A, Sharma R, Corcoran TE, Garoff S, Przybycien TM, Tilton RD. Surfactant Driven Post-Deposition Spreading of Aerosols on Complex Aqueous Subphases. 1: High Deposition Flux Representative of Aerosol Delivery to Large Airways. Journal of Aerosol Medicine and Pulmonary Drug Delivery. 2015; 28:382–393. An article which contains experimental observations of surfactant-containing aerosol deposition at high aerosol fluxes. DOI: 10.1089/jamp.2014.1168 [PubMed: 25723759]

70☆☆. Sharma R, Khanal A, Corcoran TE, Garoff S, Przybycien TM, Tilton RD. Surfactant Driven Post-Deposition Spreading of Aerosols on Complex Aqueous Subphases. 2: Low Deposition

Flux Representative of Aerosol Delivery to Small Airways. Journal of Aerosol Medicine and Pulmonary Drug Delivery. 2015; 28:394–405. An article which contains experimental observations of surfactant-containing aerosol deposition at low aerosol fluxes. DOI: 10.1089/jamp.2014.1167 [PubMed: 25757067]

71. Buboltz JT, Feigenson GW. Phospholipid Solubility Determined by Equilibrium Distribution between Surface and Bulk Phases. Langmuir. 2005; 21:6296–6301. DOI: 10.1021/la047086k [PubMed: 15982034]
72. Albrecht O, Gruler H, Sackmann E. Polymorphism of phospholipid monolayers. J Phys France. 1978; 39:301–313. DOI: 10.1051/jphys:01978003903030100
73☆. Lee KYC. Collapse mechanisms of Langmuir monolayers. Annu Rev Phys Chem. 2008; 59:771–791. A review of collapse mechanisms of lipid monolayers, relevant to delivering lipid surfactant to a pre-existing lipid layer on the lung ASL. DOI: 10.1146/annurev.physchem.58.032806.104619 [PubMed: 18393683]
74. Duncan SL, Larson RG. Comparing Experimental and Simulated Pressure-Area Isotherms for DPPC. Biophysical Journal. 2008; 94:2965–2986. DOI: 10.1529/biophysj.107.114215 [PubMed: 18199666]
75. Gopal A, Lee KYC. Morphology and Collapse Transitions in Binary Phospholipid Monolayers. J Phys Chem B. 2001; 105:10348–10354. DOI: 10.1021/jp012532n
76. Kubo I, Adachi S, Maeda H, Seki A. Phosphatidylcholine monolayers observed with Brewster angle microscopy and π-A isotherms. Thin Solid Films. 2001; 393:80–85. DOI: 10.1016/S0040-6090(01)01101-4
77. Pocivavsek L, Frey SL, Krishan K, Gavrilov K, Ruchala P, Waring AJ, Walther FJ, Dennin M, Witten TA, Lee KYC. Lateral stress relaxation and collapse in lipid monolayers. Soft Matter. 2008; 4:2019–11. DOI: 10.1039/b804611e [PubMed: 19657472]
78. Gaboriaud F, Golan R, Volinsky R, Berman A, Jelinek R. Organization and Structural Properties of Langmuir Films Composed of Conjugated Polydiacetylene and Phospholipids. Langmuir. 2001; 17:3651–3657. DOI: 10.1021/la0012790
79. Gopal A, Lee KYC. Headgroup Percolation and Collapse of Condensed Langmuir Monolayers †. J Phys Chem B. 2006; 110:22079–22087. DOI: 10.1021/jp061562t [PubMed: 17078643]
80☆☆. Fallest DW, Lichtenberger AM, Fox CJ, Daniels KE. Fluorescent visualization of a spreading surfactant. New J Phys. 2010; 12:073029–12. An article which simultaneously observes Marangoni ridge height and surfactant concentration profile during spreading. DOI: 10.1088/1367-2630/12/7/073029
81☆☆. Swanson ER, Strickland SL, Shearer M, Daniels KE. Surfactant spreading on a thin liquid film: reconciling models and experiments. Journal of Engineering Mathematics. 2015; 94:63–79. An article which compares experimentally observed Marangoni ridge height and surfactant concentration profiles directly to theoretical models. DOI: 10.1007/s10665-014-9735-0
82. Caffrey M, Hogan J. LIPIDAT: a database of lipid phase transition temperatures and enthalpy changes. DMPC data subset analysis. Chem Phys Lipids. 1992; 61:1–109. [PubMed: 1315624]
83. Gaboriaud F, Volinsky R, Berman A, Jelinek R. Temperature dependence of the organization and molecular interactions within phospholipid/diacetylene Langmuir films. Journal of Colloid and Interface Science. 2005; 287:191–197. DOI: 10.1016/j.jcis.2005.01.110 [PubMed: 15914166]
84. Lösche M, Möhwald H. Impurity controlled phase transitions of phospholipid monolayers. Eur Biophys J. 1984:35–42. [PubMed: 6468343]
85. Launois-Surpas MA, Ivanova T, Panaiotov I. Behavior of pure and mixed DPPC liposomes spread or adsorbed at the air-water interface. Colloid and Polymer Science. 1992; 270:901–911. DOI: 10.1007/BF00657735
86. Helfrich W. Blocked lipid exchange in bilayers, its possible influence on the shape of vesicles. Z Naturforsch, C, Biosci. 1974; 29C:510–515.
87. Minocchieri S, Knoch S, Schoel WM, Ochs M, Nelle M. Nebulizing poractant alfa versus conventional instillation: Ultrastructural appearance and preservation of surface activity. Pediatr Pulmonol. 2014; 49:348–356. DOI: 10.1002/ppul.22838 [PubMed: 24039226]
88. Taylor KMG, Taylor G, Kellaway IW, Stevens J. The stability of liposomes to nebulisation. International Journal of Pharmaceutics. 1990; 58:57–61.

89. Leung K, Bridges PA, Taylor K. The stability of liposomes to ultrasonic nebulisation. International Journal of Pharmaceutics. 1996; 145:95–102. DOI: 10.1016/S0378-5173(96)04730-8

90☆☆. Iasella SV, Stetten AZ, Corcoran TE, Garoff S, Przybycien TM, Tilton RD. Aerosolizing Lipid Dispersions Enables Antibiotic Transport Across Mimics of the Lung Airway Surface Even in the Presence of Pre-existing Lipid Monolayers. Journal of Aerosol Medicine and Pulmonary Drug Delivery. 2017; 30:1–9. An article which shows that aerosolized lipid dispersion can induce transport of antibiotic across biologically relevant length scales. DOI: 10.1089/jamp.2017.1412 [PubMed: 27537608]

91. Charron JR, Tilton RD. A Scanning Angle Reflectometry Investigation of Block Copolymer Adsorption to Insoluble Lipid Monolayers at the Air Water Interface. The Journal of Physical Chemistry. 1996; 100:3179–3189. DOI: 10.1021/jp9521619

92. Wu G, Majewski J, Ege C, Kjaer K, Weygand MJ, Lee KYC. Interaction between lipid monolayers and poloxamer 188: an X-ray reflectivity and diffraction study. Biophysical Journal. 2005; 89:3159–3173. DOI: 10.1529/biophysj.104.052290 [PubMed: 16100276]

93. Lewis J, Ikegami M, Higuchi R, Jobe A, Absolom D. Nebulized vs. instilled exogenous surfactant in an adult lung injury model. Journal of Applied Physiology. 1991; 71:1270–1276. [PubMed: 1757348]

94. Corcoran TE, Thomas KM, Garoff S, Tilton RD, Przybycien TM, Pilewski JM. Imaging the Postdeposition Dispersion of an Inhaled Surfactant Aerosol. Journal of Aerosol Medicine and Pulmonary Drug Delivery. 2012; 25:290–296. DOI: 10.1089/jamp.2011.0920 [PubMed: 22393908]

95. Marcinkowski AL, Garoff S, Tilton RD, Pilewski JM, Corcoran TE. Postdeposition Dispersion of Aerosol Medications Using Surfactant Carriers. Journal of Aerosol Medicine and Pulmonary Drug Delivery. 2008; 21:361–370. DOI: 10.1089/jamp.2008.0699 [PubMed: 18800882]

96. Grohmann FL, Csempesz F, Szogyi M. Stabilization of small unilamellar DMPC-liposomes by uncharged polymers. Colloid and Polymer Science. 1998; 276:66–71.

97. Keating E, Zuo YY, Tadayyon SM, Petersen NO, Possmayer F, Veldhuizen RAW. Biochimica et Biophysica Acta. BBA - Biomembranes. 2012; 1818:1225–1234. DOI: 10.1016/j.bbamem.2011.12.007 [PubMed: 22206628]

98. Lipp MM, Lee KYC, Zasadzinski JA, Waring AJ. Design and performance of an integrated fluorescence, polarized fluorescence, and Brewster angle microscope/Langmuir trough assembly for the study of lung surfactant monolayers. Rev Sci Instrum. 1997; 68:2574–10. DOI: 10.1063/1.1148163

99. Saad SMI, Policova Z, Acosta EJ, Neumann AW. Effect of surfactant concentration, compression ratio and compression rate on the surface activity and dynamic properties of a lung surfactant. Biochimica Et Biophysica Acta. 2012; 1818:103–116. DOI: 10.1016/j.bbamem.2011.10.004 [PubMed: 22020010]

100. Kumar S, Matar OK. Dewetting of thin liquid films near soft elastomeric layers. Journal of Colloid and Interface Science. 2004; 273:581–588. DOI: 10.1016/j.jcis.2003.11.044 [PubMed: 15082397]

101☆. Craster RV, Matar OK. Dynamics and stability of thin liquid films. Rev Mod Phys. 2009; 81:1131–1198. A review of instabilities that occur during Marangoni spreading events on thin liquid films with a solid substrate. DOI: 10.1103/RevModPhys.81.1131

102☆. Lee KS, Ivanova N, Starov VM, Hilal N, Dutschk V. Kinetics of wetting and spreading by aqueous surfactant solutions. Advances in Colloid and Interface Science. 2008; 144:54–65. An article on Marangoni spreading on porous and hydrophobic substrates. DOI: 10.1016/j.cis.2008.08.005 [PubMed: 18834966]

103☆. Strickland SL, Hin M, Sayanagi MR, Gaebler C, Daniels KE, Levy R. Self-healing dynamics of surfactant coatings on thin viscous films. Phys Fluids. 2014; 26:042109–25. An article which experimentally observes the self-healing of thin viscous fluids after the Marangoni ridge has deformed the interface. DOI: 10.1063/1.4872020

104. Gilbert BE, Six HR, Wilson SZ, Wyde PR, Knight V. Small particle aerosols of enviroxime-containing liposomes. Antiviral Res. 1988; 9:355–365. [PubMed: 3228281]

Highlights

- Marangoni driven flows have potential for transporting therapeutics in the lung
- Marangoni transport on simple thin liquid films is well understood
- Transport on the complex lung airway surfaces challenges these simpler models
- Transport can be achieved even in the presence of endogenous surfactant
- When aerosolized, lipids can drive Marangoni flows on surfaces mimicking the airways

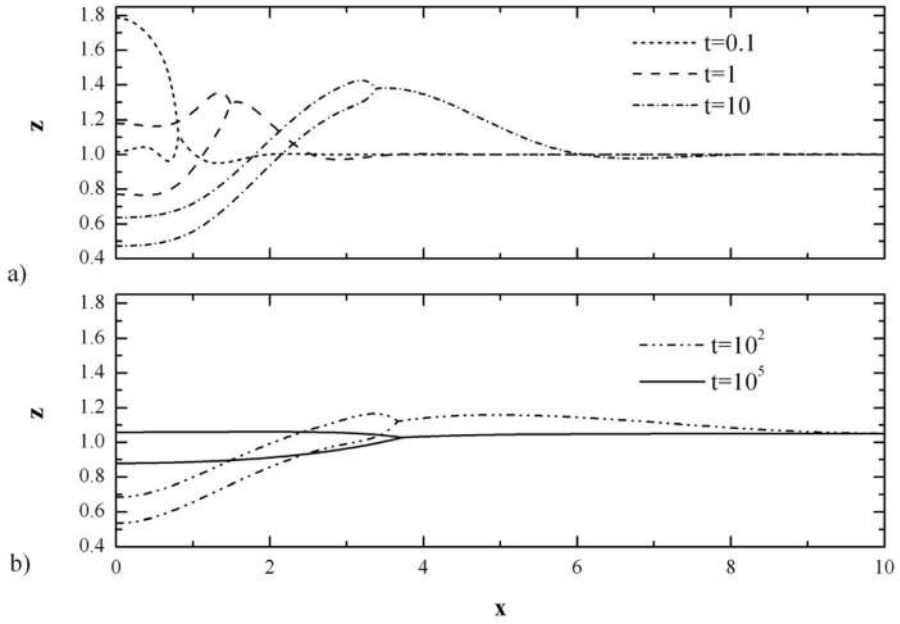

Figure 1.

Modeled spatio-temporal evolution of one drop simulation in Matar's "base case" (for a full list of parameters, please see section IV of reference [40]). This base case corresponds to a slender drop containing surfactant that is soluble in the drop (with a concentration well above the CMC) and insoluble in the subphase. This surfactant can exist as a monomer at all interfaces. The drop solvent is insoluble in the subphase. The two axes "z" and "x" represent non-dimensional vertical and horizontal spatial parameters respectively. "t" is a non-dimensional time parameter. Panels "a" and "b" are separated for clarity and "b" is simply continuation of the same simulation. The left side of the panel goes through the central axis of the drop and the drop is the closed region when the panel is reflected about the left axis. Spreading progresses towards the right. The Marangoni ridge can be most clearly seen at t = 10. Reprinted with permissions from reference [40].

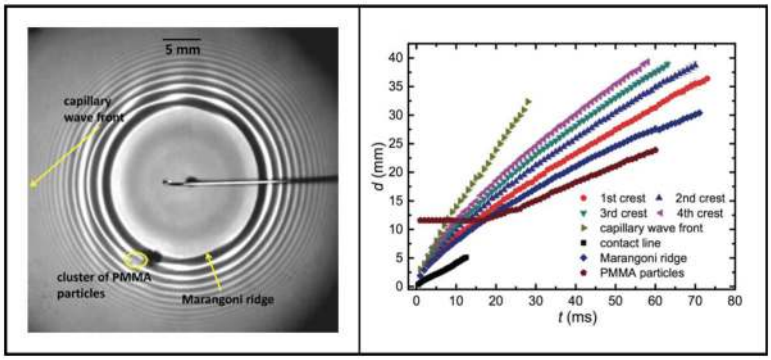

Figure 2.

The left panel shows a representative image of the spreading of a surfactant drop on a water surface. The outermost concentric rings are the capillary waves. The innermost dark ring is the Marangoni ridge. The indicator particles are circled while their shadow can be seen as a dark spot to their right. The right panel shows the position of drop contact line, capillary wave crests, Marangoni ridge, and indicator particles as a function of time. Reprinted from reference [65] with permission from Elsevier.

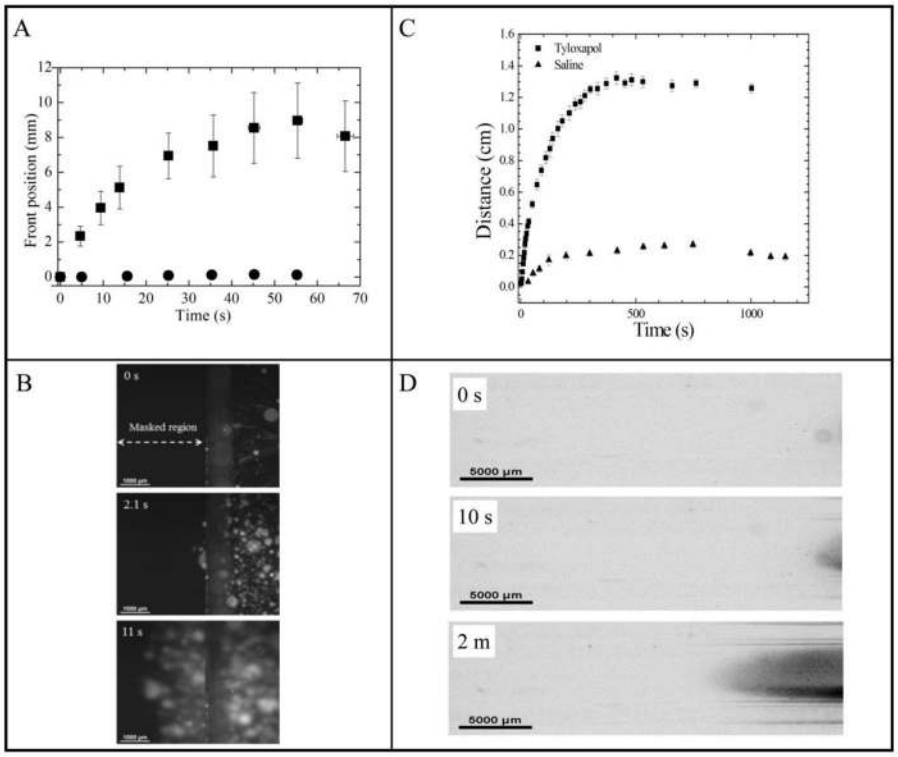

Figure 3.

A) Spreading front position versus time for a low-flux aerosol field deposited onto an aqueous poly(acrylamide) solution subphase. Circles represent the surfactant-free aerosol and squares represent a tyloxapol-containing (0.4% w/w in water) aerosol. B) Corresponding still images from the surfactant-containing aerosol case in A. Aerosol is deposited in the unmasked region to the right and spreading occurs outward into the masked region to the left. C) Spreading front position versus time for a high-flux aerosol field deposited onto an aqueous poly(acrylamide) solution subphase. Triangles represent surfactant-free aerosol and squares represent a tyloxapol-containing (0.1% w/w in water) aerosol. Please note that the y-axis represents the same physical variable as in A, but labels and units are different. D) Corresponding still images from the surfactant-containing aerosol case in C. Aerosol is deposited out of view to the right. Reprinted with permissions from references [70] (A and B) and [69] (C and D).

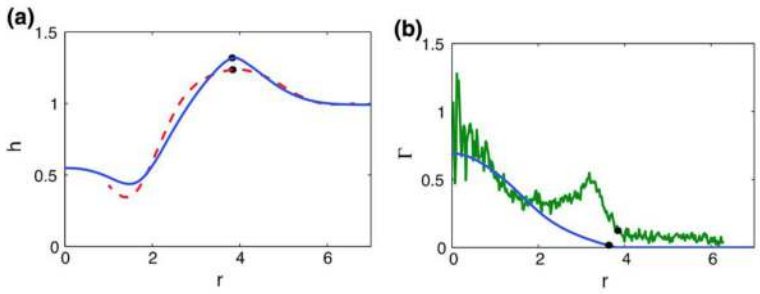

Figure 4.

a) Marangoni ridge height profile measured at 5 s in experiment (red dashed) and the corresponding numerical solution (solid blue). The bullet symbols mark the peak height in each. **b)** Surfactant concentration profiles at 5 s in experiment (noisy green) and numerical solution (smooth blue). The bullet symbols mark the surfactant leading edge in each. Data are from [80]. The small peak in intensity following the plateau in the experimental case is due to fluorescence resonance energy transfer between neighboring fluorophores and should be ignored. Reprinted from reference [81] with permission of Springer.

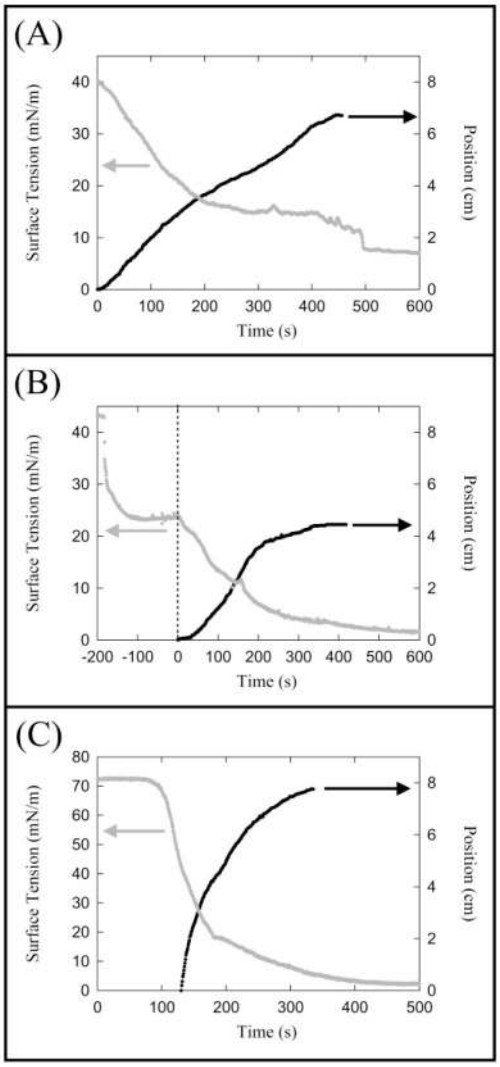

Figure 5.

Simultaneous surface tension and tracer bead motion during experiments where DPPC dispersion was aerosolized directly onto a fluid subphase. The gray line represents the surface tension measured with a Wilhelmy pin. The black represents tracer bead position at the interface with 0 cm being the edge of the confined aerosol deposition region. Subphases are (A) aqueous porcine gastric mucin solution (PGM), (B) PGM with a pre-deposited lipid monolayer, and (C) deionized water. In (B) the lipid monolayer is deposited at negative times and aerosolization begins at time t = 0. Reprinted with permission from reference [90].

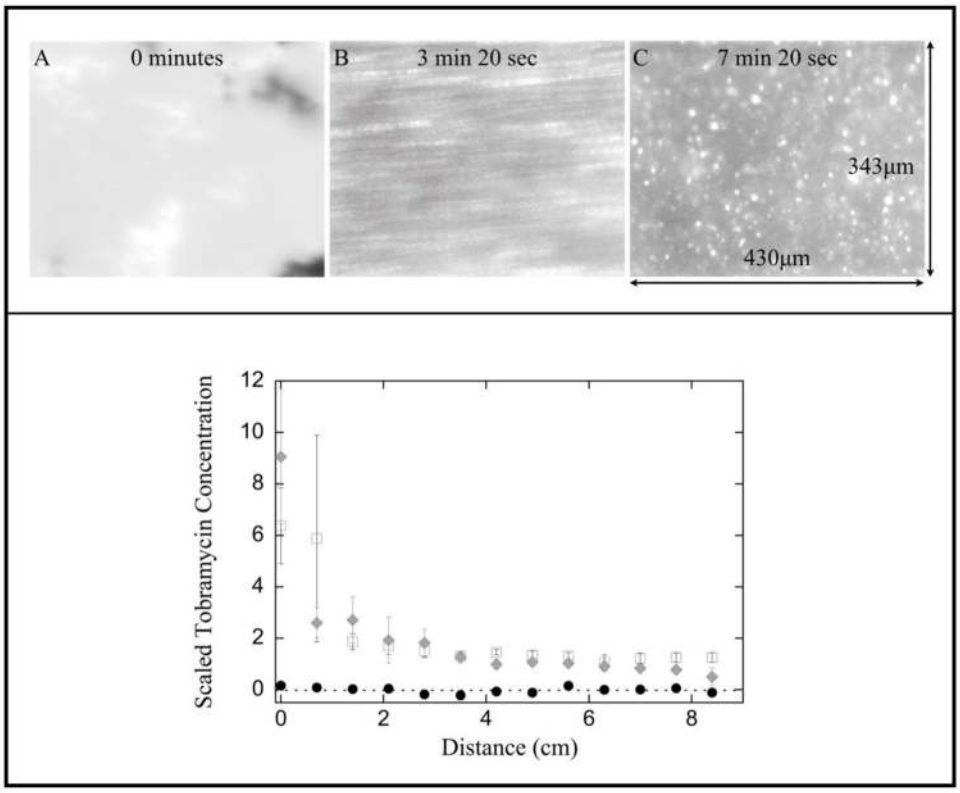

Figure 6.

The upper panel shows microscopy images of subsurface transport from experiments aerosolizing lipid dispersions directly onto water. The microscope is focused outside the region of aerosol deposition and ~ 60 μm beneath the surface. White spots are clusters of non-surface active lipid vesicles being carried beneath the surface while lipid monomer (not visible to the microscope) induces transport at the surface. (A) shows out-of-focus indicator particles at the interface before the nebulizer is turned on. (B) shows lipid clusters being transported in subsurface flow at ~ 0.05 cm/s during aerosol deposition. (C) shows the subsurface lipid clusters after spreading has ended. The lower panel (D) shows tobramycin concentration on the subphase surface in a region outside that of direct aerosolization. Cases are shown for a tobramycin solution aerosolized onto PGM (black circles), a DPPC/tobramycin mixture aerosolized onto PGM (open squares), and a DPPC/tobramycin mixture aerosolized onto a pre-deposited lipid layer on PGM (gray diamonds). The tobramycin concentration is normalized by the total deposited dose for a given run. Reprinted with permissions from references [55] (upper panel) and [90] (lower panel).